Contents lists available at ScienceDirect

Chinese Journal of Aeronautics

journal homepage: www.elsevier.com/locate/cja

Space Debris Reentry Analysis Methods and Tools

WU Ziniu[a],*, HU Ruifeng[a], QU Xi[b], WANG Xiang[b], WU Zhe[a]

[a]School of Aerospace, Tsinghua University, Beijing 100084, China

[b]China Academy of Space Technology, Beijing 100094, China

Abstract

The reentry of uncontrolled spacecraft may be broken into many pieces of debris at an altitude in the range of 75-85 km. The surviving fragments could pose great hazard and risk to ground and people. In recent years, methods and tools for predicting and analyzing debris reentry and ground risk assessment have been studied and developed in National Aeronautics and Space Administration (NASA), European Space Agency (ESA) and other organizations, including the group of the present authors. This paper reviews the current progress on this topic of debris reentry briefly. We outline the Monte Carlo method for uncertainty analysis, breakup prediction, and parameters affecting survivability of debris. The existing analysis tools can be classified into two categories, i.e. the object-oriented and the spacecraft-oriented methods, the latter being more accurate than the first one. The past object-oriented tools include objects of only simple shapes. For more realistic simulation, here we present an object-oriented tool debris reentry and ablation prediction system (DRAPS) developed by the present authors, which introduces new object shapes to 15 types, as well as 51 predefined motions and relevant aerodynamic and aerothermal models. The aerodynamic and aerothermal models in DRAPS are validated using direct simulation Monte Carlo (DSMC) method.

Keywords: space debris; reentry; ablation; breakup; risk assessment; aerodynamics

1. Introduction

The uncontrolled spacecraft like deorbited satellite and upper stage of spent rocket, reenters the Earth's dense atmosphere at the end of their life. The reentry velocity can reach more than 7 km/s, and strong aerodynamic and aerothermal loads can melt and break the structures into many pieces of debris. Inner components of the spacecraft, which can also be regarded as debris, begin their individual reentries after this breakup event. Generally, most of the debris will demise, but surviving ones can cause great risk to ground population, buildings and natural ecosystems. The

ground footprints of the surviving debris can be tens of kilometers wide and hundreds of kilometers long [1].

One of the most famous records of reentry debris experienced by human being occurred on 22 January, 1997 [2-3]. Lottie Williams, a woman in Tulsa, Oklahoma of US, was walking her dog with friends before sunrise. She watched a fireball streaking through the sky from north to south. Later, a slowly falling fragment brushed the lady's left shoulder and hit the ground with a metallic sound (top left of Fig. 1). The debris was from the second stage of the Delta rocket which was launched on 24 April, 1996. Ms. Williams might be the first person on the planet ever known to be struck by reentry debris. At the same time, a large stainless steel propellant tank landed in the front yard of a farmer near Georgetown, Texas of US (bottom of Fig. 1). And outside the town of Seguin, a titanium sphere had embedded into a field (top right of Fig. 1).

Space debris from the Earth orbit is another source of reentry debris. Since the first human astronautic

*Corresponding author. Tel.: +86-10-62784116.
E-mail address: ziniuwu@tsinghua.edu.cn

activity at 1957, there are more than 40 million man-made fragments in space now, with total mass of millions of tons [4]. Most of the space debris may pose only a minor risk on ground because of their negligible size and mass compared to large reentry spacecraft. On average, there are about 100 reentry objects each year [5]. However, there is little to be found on the ground and reported.

Fig. 1   Debris from Delta rocket second stage.

Due to the increasing requirements in astronautic applications, a fast and accurate tool for reentry prediction and ground risk assessment is needed, which becomes an important and active research area in recent years. There exist several tools for debris reentry analysis and ground risk assessment, including NASA's debris assessment software (DAS) and object reentry survival analysis tool (ORSAT), ESA's spacecraft atmosphere reentry and aerothermal breakup (SCARAB), and the recently developed reentry analysis tool debris reentry and ablation prediction system (DRAPS) by present authors.

Lips, et al. [6] classified the analysis methods into two categories: the object-oriented method and the spacecraft-oriented method. The main idea of the object-oriented method is to simplify the complicated object geometry into simple shapes like sphere, cylinder, box, etc. DAS, ORSAT and DRAPS are tools belonging to this method. The spacecraft-oriented method aims to simulate spacecraft reentry as real as possible. ESA's SCARAB [7] is the only tool of this type the authors ever known. The spacecraft-oriented method should be more accurate than the object-oriented method, but it needs more modeling efforts and computational resources because of much more complex analysis strategy. Lips, et al. [6] compared the prediction results between ORSAT and

SCARAB for a hollow sphere reentry, and showed that two tools are in good agreement. Hu. et al. [8] made comparison between DRAPS and ORSAT, confirming reasonable agreement between different tools.

The traditional object-oriented tools (DAS and ORSAT) provide very limited object shapes and aerodynamic models. For example, there are only four object shapes in DAS and ORSAT, i.e. sphere, cylinder, flat plate and box, which could be an issue for modeling debris with much more complex geometry. In the framework of the object-oriented method, one simple way is to extend object shapes and aerodynamic models naturally like what have been done for sphere, cylinder, flat plate and box in DAS and ORSAT. Based on this approach, up to 15 object shapes and relevant aerodynamic and aerothermal models have been introduced in DRAPS.

Typical debris reentry analysis tools, including DAS, ORSAT and SCARAB, are most deterministic other than probabilistic. But there exist a lot of uncertainty sources which may affect the analytical results significantly, such as initial conditions, atmospheric models, aerodynamic models and so on. In DRAPS, a simple Monte Carlo method has been integrated to account for these uncertainty effects and assess reentry risk in a probabilistic manner.

The paper is arranged as follows. In Section 2, a brief overview of typical debris reentry analysis tools is presented, including DAS, ORSAT and SCARAB. In Section 3, the object-oriented tool DRAPS developed by present authors is described on the subjects of object shapes, aerodynamic models and probabilistic analysis capability. Further discussions on breakup prediction, aerodynamic environment, and size dependence on survivability of debris reentry are given in Section 4, which may shed light on future researches on this topic of debris reentry. Overall conclusions are given in Section 5.

2. Brief Overview of Reentry Analysis Tools

2.1. Object-oriented method

DAS and ORSAT are typical tools belonging to the object-oriented method. In DAS and ORSAT [6], four types of object shapes can be modeled, i.e. sphere, cylinder, flat plate and box. Only solid objects can be modeled in DAS, while both solid and hollow ones can be analyzed in ORSAT.

Three degrees of freedom (DOF) ballistic model is commonly used for spacecraft and debris trajectory prediction in the object-oriented tools. The attitude dynamic equation of object is not directly solved but predefined as specific motion according to object shapes. For example, in ORSAT the cylinder has four motion types [6], i.e. broadside and spinning, end on and spinning, end-over-end tumbling and spinning, randomly tumbling and spinning, and the first three are schematically shown in Fig. 2. In Fig. 2, V is reentry

velocity. The aerodynamic models, aerothermal models and ablation analysis models are constructed with respect to the object shapes and predefined motions.

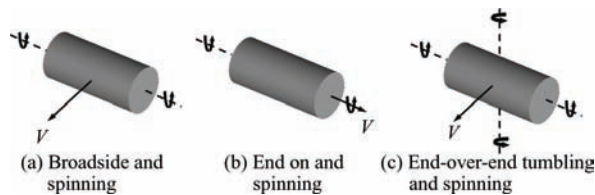(a) Broadside and spinning   (b) End on and spinning   (c) End-over-end tumbling and spinning

Fig. 2   Cylinder motion types in ORSAT.

For object with non-tumbling motion, aerodynamic forces and heating are integrated analytically by collisionless molecular kinetic theory in free molecular flow regime, Newtonian or similar engineering methods in continuum flow regime, and bridging method in transitional regime [6,8-9]. If the object is tumbling, aerodynamic forces and heating are weighted averages of values predicted by non-tumbling motion models [10].

The ablation analysis model calculates the heating rate and temperature distribution of the object, and judges whether the object is melt. In ORSAT, either zero-dimensional (lumped-mass) or one-dimensional heat conduction approach can be used for ablation analysis [6,8]. The zero-dimensional heat conduction model does not calculate temperature distribution but average temperature of the object, while the one-dimensional model solves the heat conduction equation in thickness direction. Hence, partially melting process of the object could be simulated in the one-dimensional model.

The structural analysis model is always omitted in the object-oriented method, so the breakup event cannot be directly predicted. In DAS and ORSAT, a simple altitude criterion is employed which means a spacecraft will breakup at a given altitude (78 km as default in ORSAT).

ORSAT has been used for many spacecraft reentry applications, e.g. hollow sphere comparing with ESA's SCARAB [6], barium fuel rod [11], the SPARTAN spacecraft [12], the second stages of Delta rocket [13], the UARS spacecraft [14], and so on.

2.2. Spacecraft-oriented method

In the spacecraft-oriented method, the spacecraft geometry and structure are modeled as real as possible.

In SCARAB, a complex spacecraft is composed of some subsystems, and modeled hierarchically to the final primitives, which are panelized elementary objects like sphere, cylinder, plate and box as the lowest level. Fig. 3 shows the BeppoSAX satellite geometry modeling in SCARAB [15]. There are 859 primitives in SCARAB, and 177 708 surface panels as well as 72 548 volume panels.

(a) Main structure and solar panels   (b) Inner components (courtesy of Portelli, et al.[15])
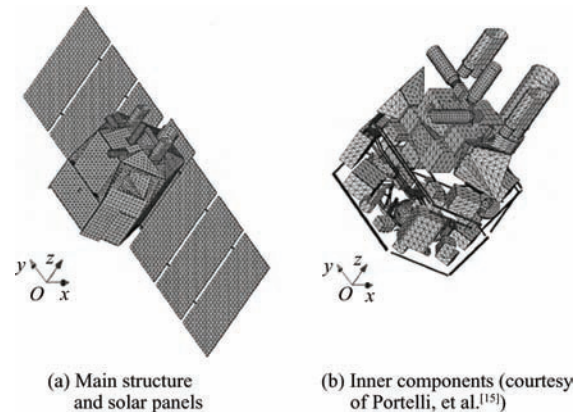
Fig. 3   BeppoSAX satellite geometry model in SCARAB.

Although the primitives are also simple shape objects, there exist apparent differences among SCARAB and the object-oriented tools. Firstly, the primitives in SCARAB are panelized surfaces or volumes while the simple shape objects in DAS and ORSAT are regarded as a whole. Secondly, in SCARAB the primitives are "installed" at the right locations with respect to other components in the way similar to reality, but in ORSAT only the logical parent/children relationship are considered and relative position relations among different components are not modeled.

The modeling of spacecraft in SCARAB can achieve very accurate level in geometry, total mass, center of gravity location and moments of inertia. For structural analysis, some "cuts" should be defined in the geometrical modeling step, at which the stress will be analyzed to judge whether breakup happens.

6 DOF model is used in spacecraft-oriented tools to obtain the position and attitude of reentry object at each instant. Aerodynamic forces and torques are integrated over all surface panels in the aerodynamic module. Local pressure and heating at each surface panel are calculated using similar methods with that in the object-oriented tools, which only need to know the freestream condition and the relative inclination between freestream and normal direction of the surface panel.

In SCARAB, two-dimensional heat conduction model is used for ablation analysis [16]. If the absorbed heat of a volume panel exceeds its maximum capacity, this panel will be melt and new fragments will generate. The stress level at the predefined cut is monitored. When exceeding maximum stress level, then the parts connected to this cut will be broken. Tewari [9] proposed a new thermomechanical breakup model to account for aerodynamic heating and centrifugal stress induced breakup.

SCARAB has been used in many astronautic applications, as automated transfer vehicle (ATV), German X-ray satellite ROSAT, the Ariane 5, the Italian satellite BeppoSAX [15], the MIR space station [17-18] (see Fig. 4), etc.
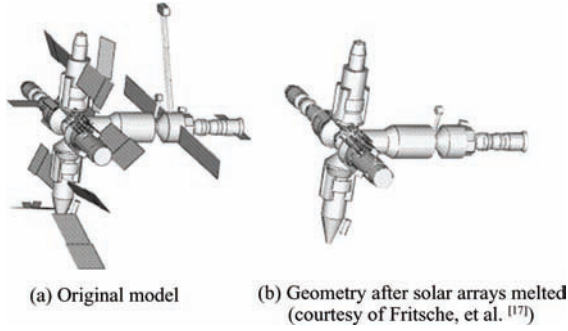
(a) Original model   (b) Geometry after solar arrays melted
(courtesy of Fritsche, et al. [17])

Fig. 4　MIR space station reentry analysis in SCARAB.

2.3. Hazard and risk assessment

In order to evaluate the hazard and ground risk due to a single surviving debris, the NASA safety standard NSS 1740.14 [19] introduces an equivalent casualty area A_{ci} of a single debris, which is composed of the cross-section area A_i of the debris and a projected human risk cross-section area of A_h=0.36 m^2,

$$A_{ci} = \sqrt{A_h} + \sqrt{A_i} \qquad (1)$$

The total casualty area A_c of a reentry event is the summation over all surviving fragments,

$$A_c = \sum_{i=1}^{n} \left(\sqrt{A_h} + \sqrt{A_i} \right)^2 \qquad (2)$$

which should be less than 8 m^2 according to NASA safety standard [19].

The total casualty probability E is a statistical measure of people may be struck by reentry debris,

$$E = \sum_{i=1}^{n} \rho_i \sigma_i A_{ci} \qquad (3)$$

where ρ_i is the population density at ground location of the ith debris, A_{ci} is the casualty area of the ith debris defined by Eq. (1), and σ_i is the probability of the ith debris impacting a specific unit area, which is given by [5,20]

$$\sigma_i(\delta, \phi) = \frac{1}{2\pi^2 R_e^2 (\sin^2 \phi - \sin^2 \delta)^{1/2}} \qquad (4)$$

where δ is the latitude of impact location, ϕ the reentry inclination angle, R_e the Earth's spherical radius. A threshold of total casualty probability E of 1:10 000 per reentry event is proposed by NASA [19], below which the reentry hazard could be accepted.

3. Debris Reentry and Ablation Prediction System

DRAPS developed by present authors falls within the category of the object-oriented method.

DRAPS adopts 3 DOF ballistic model for trajectory prediction and zero-dimensional or one-dimensional heat conduction approach for ablation analysis, which is the same as ORSAT.

Compared with ORSAT, significant improved features of DRAPS lie in new object shapes and relevant aerodynamic and aerothermal models, more reasonable breakup criteria and Monte Carlo simulation capability

for uncertainty analysis of debris reentry.

3.1. Object shapes and aerodynamic models

The object shapes are extended to 15 types in DRAPS as well as 51 predefined motions [8], including half sphere, half cylinder, cylinder with one sphere end, cylinder with two sphere ends, flat cone, sphere cone, parabolic cone, cylinder assembly, box-cylinder assembly, etc., as shown in Fig. 5.

(a) Sphere　(b) Cylinder　(c) Flat plate　(d) Box

(e) Half sphere　(f) Half cylinder　(g) Cylinder with one sphere end　(h) Cylinder with two sphere ends

(i) Flat cone　(j) Sphere cone　(k) Parabolic cone

(l) Cylinder assembly 1　(m) Cylinder assembly 2　(n) Box-cylinder assembly 1　(o) Box-cylinder assembly 2
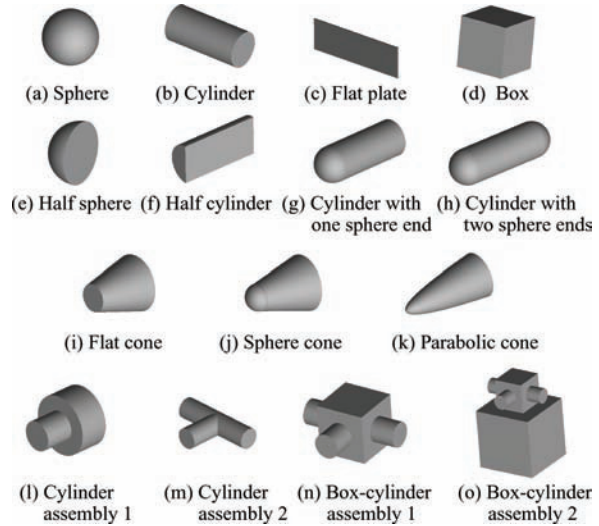
Fig. 5　Object shape types in DRAPS.

The aerodynamic and aerothermal models for each object shape and predefined motion are developed in the way similar to that for 4 basic object shapes in ORSAT. More detailed descriptions of these models could be found in Hu, et al. [8].

The model predicted drag coefficients in DRAPS to Knudsen number are plotted in Fig. 6 for cylinder, sphere cone and cylinder assembly 2. The aerodynamic properties are similar for different object shapes, i.e. the drag coefficient in continuum flow is smaller than in free molecular flow regime, and between two regimes the drag coefficient is connected smoothly by bridging method in transitional regime.
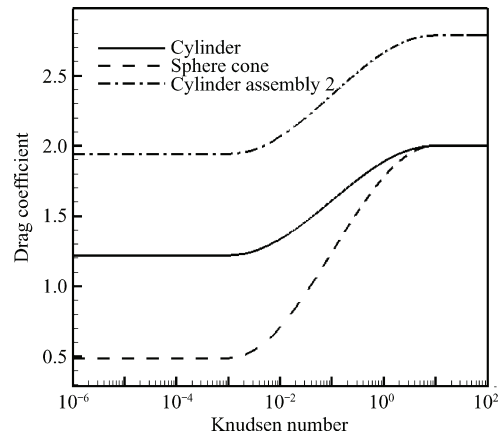

Fig. 6　Comparison of drag coefficients among cylinder, sphere cone and cylinder assembly 2.

3.2. Validation of aerodynamic models

The aerodynamic and aerothermal models should be carefully validated in order to investigate their accuracy and fidelity in reentry analysis.

In the present study, flow past a cylinder with diameter of 1 m and length of 4 m is simulated using computational fluid dynamics (CFD) and direct simulation Monte Carlo (DSMC) methods. The CFD simulation is carried out at hypersonic continuum flow condition of H=30 km, Kn=1.1×10⁻⁶, Ma=10, where H is altitude, Kn=λ/L is the Knudsen number (λ is mean free path of gas molecule, L is reference length of the object), Ma is the Mach number. DSMC simulations are performed at free molecular flow condition of H=150 km, Kn=16.5, Ma=14, and transitional flow condition of H=110 km, Kn=0.4, Ma=25. Fig. 7 shows the pressure and temperature contours of flow past

(a) *H*=30 km, pressure

(b) *H*=30 km, temperature

(c) *H*=110 km, pressure

(d) *H*=110 km, temperature

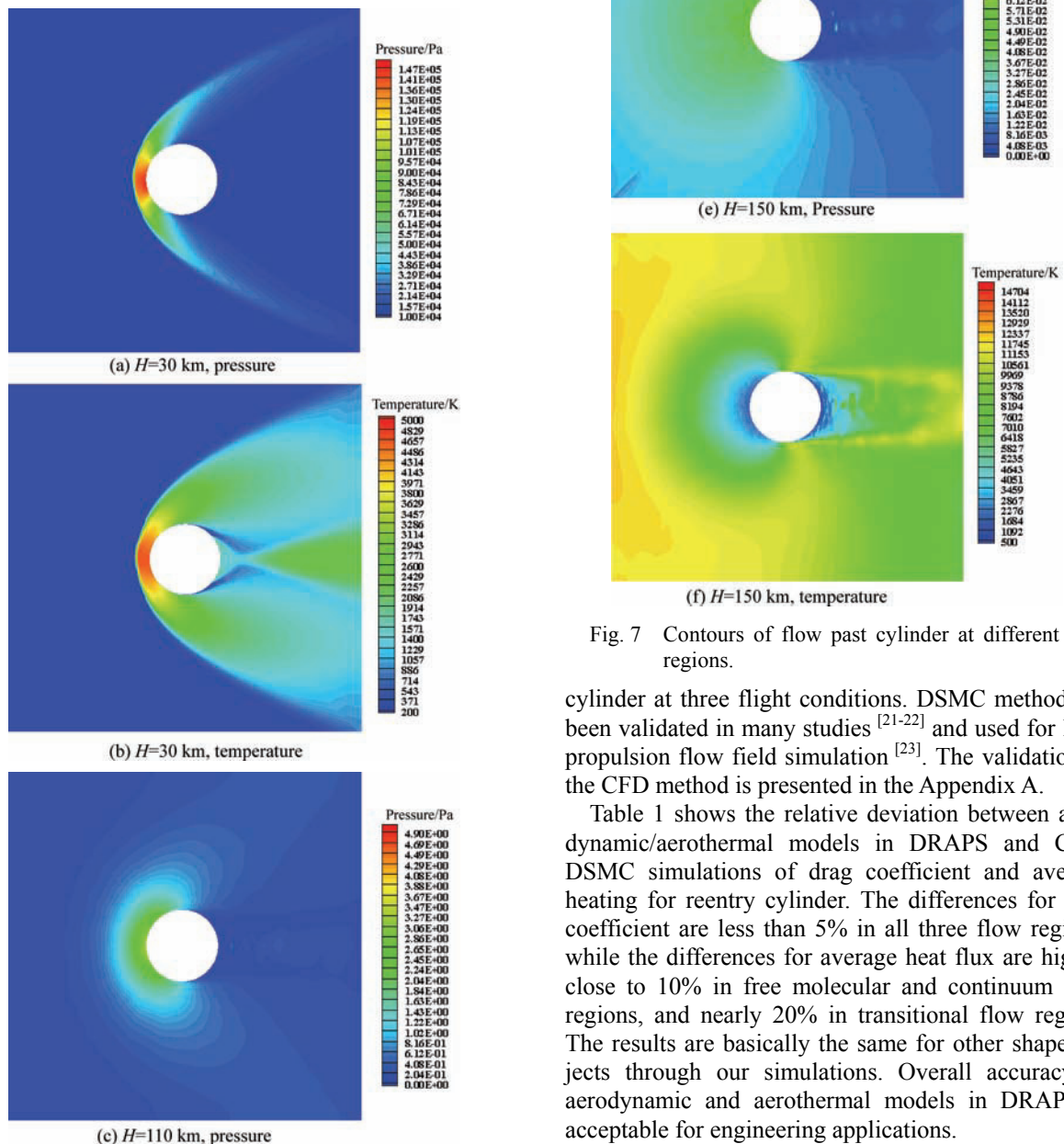(e) *H*=150 km, Pressure

(f) *H*=150 km, temperature

Fig. 7   Contours of flow past cylinder at different flow regions.

cylinder at three flight conditions. DSMC method has been validated in many studies [21-22] and used for laser propulsion flow field simulation [23]. The validation of the CFD method is presented in the Appendix A.

Table 1 shows the relative deviation between aerodynamic/aerothermal models in DRAPS and CFD/ DSMC simulations of drag coefficient and average heating for reentry cylinder. The differences for drag coefficient are less than 5% in all three flow regions, while the differences for average heat flux are higher, close to 10% in free molecular and continuum flow regions, and nearly 20% in transitional flow regime. The results are basically the same for other shape objects through our simulations. Overall accuracy of aerodynamic and aerothermal models in DRAPS is acceptable for engineering applications.

Table 1　Relative deviation between aerodynamic/ aerothermal models in DRAPS and CFD/ DSMC simulations

		%
Flow region	Drag coefficient	Average heat flux
Free molecular flow	1	5
Transitional flow	2	17
Continuum flow	1	7

3.3. Breakup prediction model

Besides the altitude criterion in ORSAT, a temperature criterion for breakup altitude prediction is used in DRAPS [8].

The temperature criterion was proposed by Baker, et al. [24], assuming that the spacecraft should break up when surface temperature reaches a given value (e.g. melting temperature). Breakup altitude prediction of the SPARTAN spacecraft reentry using temperature criterion yields good agreement with observation data [8].

3.4. Monte Carlo simulation capability

Most of the existing analysis tools for spacecraft and debris reentry analysis belong to deterministic approach which does not concern uncertainty effects.

In fact, the reentry problem is very complex and there are a lot of uncertainty sources which may affect the prediction results, such as initial conditions, atmospheric models, aerodynamic models, etc. Frank, et al. [25] ascribed the underlying uncertainty sources to the material physical properties, breakup and demise, and the prediction models. A probabilistic tool is more appropriate than deterministic one for this problem.

In DRAPS, a simple Monte Carlo module is established to account for uncertainties from initial conditions for single reentry object. Fig. 8 shows the possible landing area for a single reentry hollow sphere from Monte Carlo simulation.
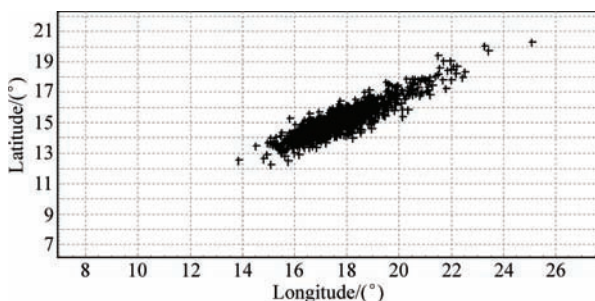

Fig. 8　Possible landing area for a single reentry hollow sphere from Monte Carlo simulation.

4. Further Discussion

In spite of significant improvements in debris reentry analysis method and tools development, there are some issues which are still not well understood and resolved. Breakup prediction is the most important one.

Moreover, some preliminary studies, such as aerodynamic environment for reentry debris and size dependence on debris survivability, could be helpful and useful to construct more reasonable prediction models or reduce computation efforts.

4.1. Breakup prediction method

Unlike the controlled and manned vehicles like space shuttle and reentry capsule, the unmanned and uncontrolled reentry spacecraft like satellite usually encounters a breakup event commonly at an altitude in the range between 75 km and 85 km [5]. Typical trajectories of reentry spacecraft with breakup and generated debris are illustrated in Fig. 9.
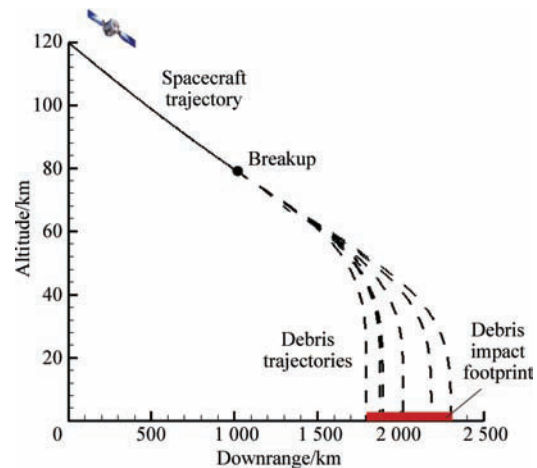

Fig. 9　Trajectories of reentry spacecraft and debris.

The spacecraft begins reentry due to the atmospheric drag after long-term in-orbit flight. High reentry velocity as well as increasing atmospheric density would impose severe aerodynamic and aerothermal loads on the spacecraft. Breakup event happens when the loads exceed the limits of the structure. Then the spacecraft breaks into many pieces of debris including exposed inner components.

Traditional altitude criterion based on long-term observation and statistics for breakup prediction in object-oriented tools is empirical. The temperature criterion is more reasonable due to the consideration of some physical factors, but is still empirical and inaccurate.

In the spacecraft-oriented method, the stress and heating at predefined "cuts" are monitored to judge whether breakup happens. This method is much more accurate than the breakup criteria in the object-oriented tools, but at some particular circumstances it also cannot simulate the real situation because of inappropriate aerodynamic and aerothermal models.

Current aerodynamic and aerothermal models in continuum flow regime are suitable for hypersonic flow past clean blunt object, where only a detached

shock wave exists away from the object. However, for complex spacecraft or multi-object systems, the shock wave interaction phenomenon may appear [26], which could induce high pressure and heating regions and the ablation and breakup process may be significantly altered. It might be difficult to consider these effects in current fast analysis tools and further studies are needed.

4.2. Aerodynamic environment for debris reentry

The aerodynamic environment, which includes key aerodynamic parameters and flow properties at reentry condition, is helpful for preliminary consideration of the aerodynamic and aerothermal models. Hu, et al. [27] constructed a velocity-altitude map (V-A map for short) for analyzing the aerodynamic environment of hypersonic vehicles. In the V-A map, various aerodynamic parameters as Reynolds number, Mach number, Knudsen number are displayed quantitatively, and different flow regions as laminar/unstable/turbulent flow regimes, rarefaction/continuum flow regions could be identified intuitively.

In Fig. 10, we superimpose the reentry trajectory of an aluminum hollow sphere (1 m in diameter, 30 mm in thickness) on the contour lines of $Ma=5$ and 15, $Re=10^3$ and 10^6, and $Kn=0.001$ and 10 in the V-A map. The characteristic length for Reynolds number and Knudsen number is the sphere diameter. During the whole reentry course, Knudsen number is below 0.001, Reynolds number lies in the range between 10^3 and 10^6, and Mach number decreases from more than 15 to near 0, which entirely covers the hypersonic, supersonic and subsonic flow regimes.
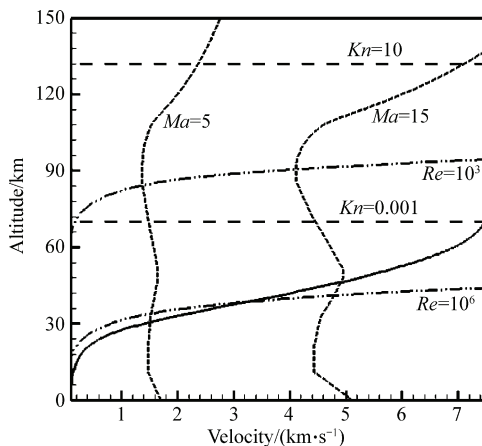

Fig. 10   Contour lines of non-dimensional flow parameters and sphere reentry trajectory (solid line).

For rarefaction effect, the flow field can be roughly classified into continuum flow ($Kn<0.001$), transitional flow ($0.1<Kn<10$) and free molecular flow ($Kn>10$) [28]. For stability and transition, the flow field can be laminar flow, unstable flow or turbulent flow. In Fig. 11, the trajectory of the reentry sphere is superimposed on the edges of different flow regimes. The critical lines in Fig. 11 which distinguishes lami-

nar/unstable/turbulent flow regions, are based on linear stability computations for a flat plate with unit length [29-30]. In the preliminary analysis, we could qualitatively know that the flow field around the reentry sphere is continuum and laminar, and the stagnation heat flux is at an order of 100 kW/m^2 above 50 km.
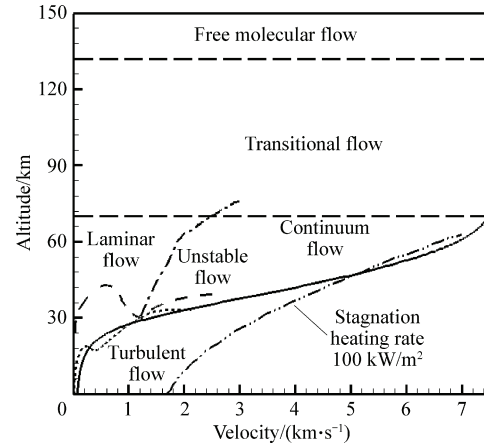

Fig. 11   Flow regions and sphere reentry trajectory (solid line).

4.3. Size dependence on debris survivability

Koppenwaller, et al. [31] analyzed the survivability of simple shape solids as function of their sizes.

In Fig. 12, the demise altitudes of reentry solid spheres with different materials and diameters are presented. For a given material, there exists a minimum and maximum diameter between which the sphere cannot survive to ground. Below the minimum diameter, the reentry velocity of the object decreases quickly at high altitude due to large area-to-mass ratio, so that it could survive because of the low aerodynamic heating level (proportional to cubic of the reentry velocity). Above the maximum diameter, the heat storage capacity of the reentry object is large enough to allow the survival.
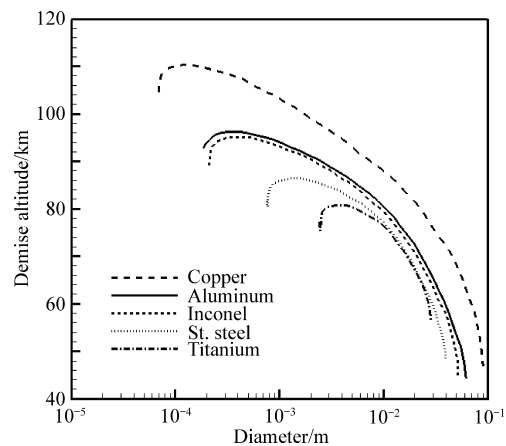

Fig. 12   Demise altitude of reentry solid spheres with different materials and diameters (courtesy of Koppenwaller, et al. [31]).

Fritsche, et al. [32] analyzed the demise limits of hollow reentry objects (sphere, box and cylinder) using analysis method, and obtained the demise regions with respect to object size and wall thickness. The size dependence of hollow objects is similar to solid ones.

The hazard of surviving reentry objects with small size could be omitted, while large size ones should be analyzed carefully. Therefore, it is useful to establish a database including critical sizes for surviving debris with various shapes and materials. In astronautic applications, only large objects are analyzed which could significantly reduce the modeling work in preliminary analysis.

5. Conclusions

(1) The debris reentry analysis methods can be categorized into object-oriented and spacecraft-oriented methods. The spacecraft-oriented method is more accurate than the object-oriented approach but the computational costs are more expensive.

(2) The debris reentry analysis tool DRAPS developed by present authors introduces new object shapes to 15 types, as well as 51 predefined motions and relevant aerodynamic and aerothermal models. The aerodynamic and aerothermal models in DRPAS are validated carefully, which are at an order of 10% away from accurate numerical simulation results. A simple Monte Carlo method is adopted for single object reentry uncertainty analysis in DRAPS. In the future, more rigorous probabilistic analysis method for an entire reentry spacecraft should be developed.

(3) Current breakup prediction models need further improvements. Complex flow phenomenon like shock wave interaction may exist but not modeled in existing analysis tools, which may greatly influence the breakup event.

(4) The aerodynamic environment of debris reentry is near continuum and laminar flow at common conditions. The survivability of debris with particular shape and material is largely dependent on its size. For debris of size below a critical value, the reentry analysis work can be reduced because the object would be burned out during its reentry.

References

[1]　Klinkrad H. Space debris: models and risk analysis. Chichester: Praxis Publishing Ltd, 2006; 241-287.

[2]　Oberg J E. The things that fell to the earth. Air & Space Magazine 2005(1): 50-56.

[3]　Ailor W, Bonaparte L, Shelton A F. A strategy for reducing hazards from reentry debris. AIAA-2006-6379, 2006.

[4]　Du H, Zhang W X, Pang B J, et al. Space debris. Beijing: China Astronautic Publishing House, 2007; 1-128. [in Chinese]

[5]　Ailor W H, Patera R P. Spacecraft re-entry strategies: meeting debris mitigation and ground safety requirements. Proceedings of the Institution of Mechanical Engineers, Part G: Journal of Aerospace Engineering 2007; 221(6): 947-953.

[6]　Lips T, Fritsche B. A comparison of commonly used re-entry analysis tools. Acta Astronautica 2005; 57(2-8): 312-323.

[7]　Lips T, Fritsche B, Koppenwallner G, et al. Spacecraft destruction during re-entry—latested results and development of the SCARAB software system. Advances in Space Research 2004; 34(5): 1055-1060.

[8]　Hu R F, Wu Z N, Qu X, et al. Debris reentry and ablation prediction and ground risk assessment system. Acta Aeronautica et Astronautica Sinica 2011; 32(3): 390-399. [in Chinese]

[9]　Tewari A. Entry trajectory model with thermomechanical breakup. Journal of Spacecraft and Rockets 2009; 46(2): 299-306.

[10]　Klett R D. Drag coefficients and heating ratios for right circular cylinders in free-molecular and continuum flow from Mach 10 to 30. Sandia Corporation, SC-RR-64-2141, 1964.

[11]　Rochelle W C, Kirk B S, Ting B C, et al. Modeling of space debris reentry survivability and comparison of analytical methods. 50th International Astronautical Congress. IAA-99-IAA.6.7.03, 1999.

[12]　Bouslog S A, Ross B P, Madden C B. Space debris reentry risk analysis. AIAA-1994-591, 1994.

[13]　Rochelle W, Kinsey R E, Reid E A, et al. Spacecraft orbital debris reentry aerothermal analysis. Proceedings of the Eighth Annual Thermal and Fluids Analysis Workshop: Spacecraft Analysis and Design. Houston: NASA/Johnson Space Center, 1997; 1-14.

[14]　Rochelle W C, Marichalar J J, Johnson N L. Analysis of reentry survivability of UARS spacecraft. Advances in Space Research 2004; 34(5): 1049-1054.

[15]　Portelli C, Salotti L, Anselmo L, et al. BeppoSAX equatorial uncontrolled re-entry. Advances in Space Research 2004; 34(5): 1029-1037.

[16]　Fritsche B, Klinkrad H, Kashkovsky A, et al. Spacecraft disintegration during uncontrolled atmospheric re-entry. Acta Astronautica 2000; 47(2-9): 513-522.

[17]　Fritsche B, Koppenwallner G. Computation of destructive satellite re-entries. 3rd European Conference on Space Debris. 2001; 527-532.

[18]　Fritsche B. Note on the application of SCARAB to the MIR re-entry. Proceedings of the international workshop on MIR deorbit. 2002; 99-102.

[19]　Anonymous. NSS 1740.14 NASA safety standard—guidelines and assessment procedures for limiting orbital debris. Washington, D. C.: NASA, Office of Safety and Mission Assurance, 1995; 1-67.

[20]　Patera R P. Hazard analysis for uncontrolled space vehicle reentry. AIAA-2006-6500, 2006.

[21]　Zhuang L S. Numerical simulation of flow field of air-breathing mode laser thruster for continuum and rarefied environment. Master thesis, Tsinghua University, 2006. [in Chinese]

[22]　Xu S S. Numerical simulation of flows for vehicle flying in the transitional regime. PhD thesis, Tsinghua University, 2008. [in Chinese]

[23]　Xu S S, Wu Z N, Li Q, et al. Hybrid continuum/DSMC computation of rocket mode lightcraft flow in near space with high temperature and rarefaction effect. Computers & Fluids 2009; 38(7): 1394-1404.

[24]　Baker R L, Weaver M A, Moody D M, et al. Orbital spacecraft reentry breakup. 50th International Astro-

nautical Congress. IAA-99-IAA.6.7.04, 1999.

[25] Frank M V, Weaver M A, Baker R L. A probabilistic paradigm for spacecraft random reentry disassembly. Reliability Engineering and System Safety 2005; 90(2-3): 148-161.

[26] Wang X X, Hu R F, Wu Z N. Special near space aerodynamics. Nearspace Science & Engineering 2009; 1(1): 34-42. [in Chinese]

[27] Hu R F, Wu Z N, Wu Z, et al. Aerodynamic map for soft and hard hypersonic level flight in near space. Acta Mechanica Sinica 2009; 25(4): 571-575. [in Chinese]

[28] Tsien H S. Superaerodynamics. Journal of the Aeronautical Sciences 1946; 13: 653-664.

[29] Özgen S, Kırcalı S A. Linear stability analysis in compressible, flat-plate boundary-layers. Theoretical and Computational Fluid Dynamics 2008; 22(1): 1-20.

[30] Mack L M. Linear stability theory and the problem of supersonic boundary-layer transition. AIAA Journal 1975; 13(3): 278-289.

[31] Koppenwaller G, Fritsche B, Lips T. Survivability and ground risk potential of screws and bolts of disintegrating spacecraft during uncontrolled re-entries. 3rd European Conference on Space Debris. 2001; 533-539.

[32] Fritsche B, Lips T, Koppenwaller G. Analytical and numerical re-entry analysis of simple-shaped objects. Acta Astronautica 2007; 60(8-9): 737-751.

[33] Holden M S, Wieting A R, Moselle J R, et al. Studies of aerothermal loads generated in regions of shock/ shock interactions in hypersonic flow. AIAA-1988-477, 1988.

[34] Pan S, Feng D H, Ding G H, et al. Grid dependency and convergence of hypersonic aerothermal simulation. Acta Aeronautica et Astronautica Sinica 2010; 31(3): 493-499. [in Chinese]

**Appendix A: Validation of CFD Method**

The governing equations for fluid flow past reentry debris are compressible Navier-Stokes (N-S for short) equations. The numerical solutions are obtained by solving the N-S equations in the conservative form using finite volume method. The inviscid fluxes are calculated by Roe scheme with van-Leer limiter and the viscous fluxes by central difference scheme to second order.

The hypersonic flow past cylinder is calculated to validate the CFD method [33]. The diameter of the cylinder is $d=0.038\ 1$ m, with freestream Mach number $Ma=8.0$, static pressure $p=855$ Pa, total temperature $T_0=1\ 726$ K and wall temperature $T_w=294$ K.

The numerical results, especially the heat flux on the wall, are very sensitive to the grid Reynolds number Re_g, in which the characteristic length is the size of the first grid cell away from the wall. Pan, et al. [34] found that when Re_g is smaller than 100, the CFD results could agree well with experiment. In present study, Re_g

is 10 in all cases.

In Fig. A1, comparisons between CFD and experimental results are shown for pressure coefficient and Standon number (non-dimensional heat flux) distributions on the cylinder surface. Excellent agreements between CFD and experiment are obtained which confirms the validity of current CFD method.
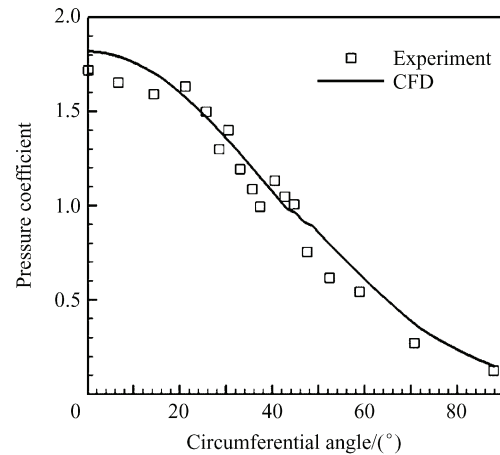
(a)
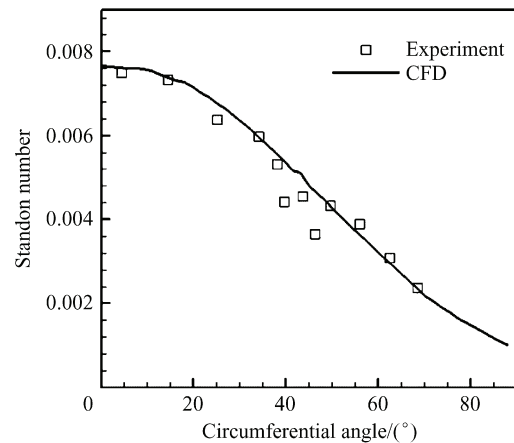
(b)

Fig. A1 Comparisons of pressure coefficient and heat flux distribution between CFD and experimental results.

Biographies:

WU Ziniu Born in 1963, he is a professor in Tsinghua University. His main research interests are fluid mechanics and aerodynamics.
E-mail: ziniuwu@tsinghua.edu.cn

HU Ruifeng Born in 1984, he is a Ph.D. student in Tsinghua University. His main research interest is aerodynamics.
E-mail: hudf03@mails.tsinghua.edu.cn